PHYSICAL REVIEW D **92,** 083006 (2015)

Effects of strong magnetic fields and rotation on white dwarf structure

B. Franzon* and S. Schramm†

Frankfurt Institute for Advanced Studies, Ruth-Moufang-1 60438 Frankfurt am Main, Germany

(Received 27 July 2015; published 14 October 2015)

In this paper we compute models for relativistic white dwarfs in the presence of strong magnetic fields. These models possibly contribute to superluminous SNIa. With an assumed axisymmetric and poloidal magnetic field, we study the possibility of the existence of super-Chandrasekhar magnetized white dwarfs by solving numerically the Einstein-Maxwell equations, by means of a pseudospectral method. We obtain a self-consistent rotating and nonrotating magnetized white dwarf model. According to our results, a maximum mass for a static magnetized white dwarf is 2.13 $M_\odot$ in the Newtonian case, and 2.09 $M_\odot$ when taking into account general relativistic effects. Furthermore, we present results for rotating magnetized white dwarfs. The maximum magnetic field strength reached at the center of white dwarfs is of the order of 10^{15} G in the static case, whereas for magnetized white dwarfs, rotating with the Keplerian angular velocity, it is of the order of 10^{14} G.

DOI: 10.1103/PhysRevD.92.083006 PACS numbers: 97.20.Rp, 97.10.Ld

I. INTRODUCTION

White dwarfs (WDs) are stellar remnants of stars with masses of up to several solar masses. With a mass comparable to that of the Sun $\sim 2 \times 10^{33}$ g, which is distributed in a volume comparable to that of the Earth, the central mass density in these objects can reach values of about 10^{11} g/cm^3. Together with neutron stars and black holes, they are end points of stellar evolution and play a key role in astrophysics [1,2].

The existence of white dwarfs was one of the major puzzles in astrophysics until Fowler [3], based on the quantum-statistical theory developed by Fermi and Dirac [4,5], showed that white dwarfs are supported by the pressure of a degenerate electron gas. In addition, Chandrasekhar in Ref. [6] found that there is a limit in the stellar mass, beyond which degenerate white dwarfs are unstable. This critical mass is the so-called *Chandrasekhar limit* and is about 1.4 $M_\odot$.

White dwarfs are mostly composed of electron-degenerate matter. The mass of the star is essentially given by the total mass of the nuclei, whereas the main contribution to the pressure is produced by the electrons. For typical WDs, thermonuclear reactions terminate at lighter nuclei, like carbon, helium, or oxygen [2,7].

Some white dwarfs are also associated with strong magnetic fields. Observations show that the surface magnetic field of these stars can reach values from 10^6 G to 10^9 G [8–12]. However, the internal magnetic field in magnetic stars is very poorly constrained by observations and can be much stronger than the one at the surface. For example, white dwarfs might have internal magnetic fields as large as $10^{12–16}$ G according to Refs. [1,13,14]. Moreover, self-consistent calculations of strongly magnetized neutron stars have suggested that the stars can possess central magnetic fields as large as 10^{18} G [15–18]. Therefore, the overall task of understanding and estimating magnetic fields inside compact objects is one of the key problems in astrophysics.

Motivated by observations of a thermonuclear supernova, which appears to be more luminous than expected (e.g. SN 2003fg, SN 2006gz, SN 2007if, SN 2009dc), it has been argued [19–23] that the progenitor of such a supernova should be a white dwarf with mass above the well-known Chandrasekhar limit, in other words, a super-Chandrasekhar white dwarf.

Progenitors with masses $M > 2.0\ M_\odot$ were considered in the literature as a result of a merger of two massive white dwarfs, or alternatively due to fast rotation [24]. In addition, super-Chandrasekhar white dwarfs were investigated in a strong magnetic field regime as in Refs. [25–27]. In the Newtonian framework, models for white dwarfs including magnetic fields and/or rotation were investigated in a series of papers [28–31]. Recently, a study of differentially rotating and magnetized white dwarfs, performed within the ideal magnetohydrodynamic regime, has shown that differential rotation might increase the mass of magnetized white dwarfs up to 3.1 $M_\odot$ [32].

Previous studies showed that magnetic white dwarfs can have their masses increased up to 2.58 $M_\odot$ for a magnetic field strength of 10^{18} G at the center of the star [26]. Nonetheless, such an approach violates not only macrophysics aspects, as for example, the breaking of spherical symmetry due to the magnetic field, but also microphysics considerations, which are relevant for a self-consistent calculation of the structure of these objects [33–35]. Besides, a self-consistent Newtonian structure calculation of strongly magnetized white dwarfs has shown that these stars exceed the traditional Chandrasekhar mass limit

*franzon@fias.uni-frankfurt.de
†schramm@fias.uni-frankfurt.de

significantly ($M \sim 1.9\ M_\odot$) for a maximum field strength of the order of 10^{14} G [14].

In this paper, we model static and rotating magnetized white dwarfs in a self-consistent way by solving Einstein-Maxwell equations in the same way as it was originally done for neutron stars in Refs. [15,36]. We also follow our recent work on highly magnetized hybrid stars [18], where both general relativistic effects and the anisotropy of the energy momentum tensor caused by the magnetic field were taken into consideration to calculate the star structure. The presence of such a strong magnetic field can locally affect the microphysics of the stellar matter, as for example, due to Landau quantization. However, as shown in Ref. [14], Landau quantization does not affect the global properties of white dwarfs. Furthermore, the authors in Ref. [14] solved the structure equations in a Newtonian form, but, as we will see, effects of general relativity are essential for determining the maximum mass of such highly magnetized white dwarfs.

Globally, the magnetic field can affect the structure of WDs since it contributes to the Lorenz force, which acts against gravity. In addition, it contributes also to the structure of spacetime, since the magnetic field is now a source for the gravitational field through the Maxwell energy-momentum tensor. In the following, as we are interested in global effects that magnetic fields and the rotation can induce in WDs, we simplify the discussion assuming white dwarfs that are predominately composed by ^{12}C ($A/Z = 2$) in an electron background.

II. BASIC EQUATIONS AND FORMALISM

In this paper, we consider rotating and nonrotating magnetized white dwarfs. In this context, the formalism used here was first applied to rotating and nonrotating magnetized neutron stars in Refs. [15,16,36], and more recently in Ref. [18]. Details of the gravitational equations, numerical procedure and other properties of the equations can be found in the references cited above and in Ref. [37]. For the sake of completeness and readability, we present the basic electromagnetic equations that, together with the gravitational equations, are solved numerically. The energy-momentum tensor of the system reads

$$T_{\alpha\beta} = (e+p)u_\alpha u_\beta + p g_{\alpha\beta} + \frac{1}{\mu_0}\left(F_{\alpha\mu}F^\mu_\beta - \frac{1}{4}F_{\mu\nu}F^{\mu\nu}g_{\alpha\beta}\right), \tag{1}$$

with $F_{\alpha\mu}$ being the antisymmetric Faraday tensor defined as $F_{\alpha\mu} = \partial_\alpha A_\mu - \partial_\mu A_\alpha$, where A_μ is the electromagnetic four-potential. The system energy density is e, the isotropic contribution to the pressure is denoted by p, the fluid velocity is given by u_α, and the metric tensor is $g_{\alpha\beta}$. The first term in Eq. (1) represents the isotropic matter contribution to the energy momentum tensor, while the second term is the anisotropic electromagnetic field contribution. Due to the symmetry of the system, a polar-spherical type coordinate system is chosen (for a review see Ref. [37]):

$$\begin{aligned} ds^2 &= -N^2dt^2 + \Psi^2 r^2 \sin^2\theta(d\phi - N^\phi dt)^2 \\ &\quad + \lambda^2(dr^2 + r^2 d\theta^2), \end{aligned} \tag{2}$$

with N, N^ϕ, Ψ and λ being functions of the coordinates (r, θ). The electromagnetic contribution (EM) to the energy-momentum tensor is obtained within the so-called $3+1$ decomposition [36,37]. The energy density becomes

$$E^{(EM)} = \frac{1}{2\mu_0}(E^iE_i + B^iB_i), \tag{3}$$

and the momentum-density flux can be written as

$$J_\phi^{(EM)} = \frac{\lambda^2}{\mu_0}(B^rE^\theta - E^rB^\theta). \tag{4}$$

The stress 3-tensor components are given by

$$S^{(EM)r}_{\ \ r} = \frac{1}{2\mu_0}(E^\theta E_\theta - E^rE_r + B^\theta B_\theta - B^rB_r), \tag{5}$$

$$S^{(EM)\theta}_{\ \ \theta} = \frac{1}{2\mu_0}(E^rE_r - E^\theta E_\theta + B^rB_r - B^\theta B_\theta), \tag{6}$$

$$S^{(EM)\phi}_{\ \ \phi} = \frac{1}{2\mu_0}(E^iE_i + B^iB_i), \tag{7}$$

being the electric field components, as measured by the Eulerian observer $\mathcal{O}_0$, written as [38]

$$E_\alpha = \left(0, \frac{1}{N}\left[\frac{\partial A_t}{\partial r} + N^\phi \frac{\partial A_\phi}{\partial r}\right], \frac{1}{N}\left[\frac{\partial A_t}{\partial \theta} + N^\phi \frac{\partial A_\phi}{\partial \theta}\right], 0\right), \tag{8}$$

and the magnetic field given by

$$B_\alpha = \left(0, \frac{1}{\Psi r^2 \sin\theta}\frac{\partial A_\phi}{\partial \theta}, -\frac{1}{\Psi \sin\theta}\frac{\partial A_\phi}{\partial r}, 0\right), \tag{9}$$

with A_t and A_ϕ the two nonzero components (for a poloidal magnetic field) of the electromagnetic four-potential $A_\mu = (A_t, 0, 0, A_\phi)$. As in Ref. [36], the equation of motion ($\nabla_\mu T^{\mu\nu} = 0$) reads

$$H(r,\theta) + \nu(r,\theta) - \ln\Gamma(r,\theta) + M(r,\theta) = \text{const}, \tag{10}$$

with $H(r,\theta)$ being the logarithm of the dimensionless relativistic enthalpy per baryon:

$$H \coloneqq \ln\left(\frac{e+p}{m_b n_b c^2}\right), \tag{11}$$

where $m_b = 1.66 \times 10^{-27}$ kg is the mean baryon mass and n_b is the baryon number density. The second term in Eq. (10) is defined as $\nu = \nu(r,\theta) \coloneqq ln(N)$, the Lorenz factor Γ is written as $\Gamma = (1-U^2)^{-\frac{1}{2}}$, the physical fluid velocity U in the ϕ direction is given by

$$U = \frac{\Psi r \sin\theta}{N}(\Omega - N^{\phi}), \tag{12}$$

and the magnetic potential $M(r,\theta)$ associated to the Lorentz force becomes

$$M(r,\theta) = M(A_{\phi}(r,\theta)) \coloneqq -\int_{A_{\phi}(r,\theta)}^{0} f(x)\mathrm{d}x, \tag{13}$$

with $f(x)$ being a current function as defined in Ref. [36] [see Eq. (5.29)]. In this paper, we use a current function $f(x) = f_0 =$ const, which is proportional to the intensity of the magnetic field, i.e., with a larger current function f_0, the magnetic field in the star increases proportionally. As shown in Ref. [15], other choices are possible for $f(x)$, however, they do not alter the conclusions.

III. MASS-RADIUS DIAGRAM FOR STATIC HIGHLY MAGNETIZED WHITE DWARFS

In this section we present the mass-radius (MR) diagram for static magnetized white dwarfs. The relation between mass and radius of nonmagnetized white dwarfs was first determined by Chandrasekhar [7]. Recently, studies of modified mass-radius relations of magnetic white dwarfs were proposed, for example, in Refs. [14,25,39]. As we also found in this work, these authors show that the mass of white dwarfs increases in the presence of magnetic fields.

In Fig. 1, we show the isocontours in the (x,z) plane of the poloidal magnetic field lines for a static star with central enthalpy of $H_c = 0.0063c^2$. As we will see in Fig. 4, this value of the enthalpy results in the maximum gravitational mass of relativistic, static and magnetized white dwarfs achieved with the code, namely, 2.09 $M_{\odot}$, which corresponds to a central mass density of 2.79×10^{10} g/cm^3. It is known that at sufficiently high densities reactions as inverse β-decay or pycnonuclear fusion can take place in the interior of white dwarfs [34,40]. As estimated in Ref. [40], for the maximum mass configuration obtained in this paper, i.e., for a central magnetic field of 1.03×10^{15} G, the onset of electron capture by carbon-12 nuclei is 4.2×10^{10} g/cm^3 with electron-ion interactions, and 3.9×10^{10} g/cm^3 without electron-ion interactions. Therefore, in our calculation, the maximum mass density reached by the most massive and nonrotating magnetized white dwarf lies below the threshold density for the onset of electron captures by carbon-12 nuclei as calculated in Ref. [40].

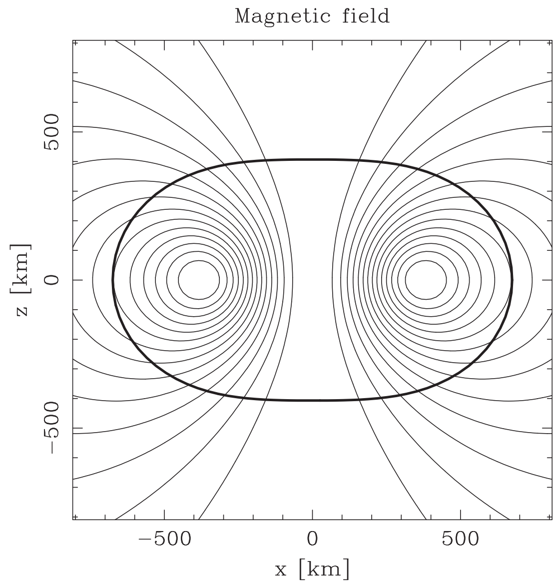

FIG. 1. Isocontours of the magnetic field strength in the (x,z) plane, with a gravitational mass of 2.09 $M_{\odot}$ and a magnetic dipole moment of 1.30×10^{34} Am^2. The ratio between the magnetic pressure and the matter pressure at the center of the star is about 1, and the magnetic field at the center reaches 1.03×10^{15} G.

In Fig. 2, we show the mass density distribution for the same star as in Fig. 1. As expected, the mass density is not spherically distributed and the maximum mass density is not at the center of the star anymore. In this case, the central magnetic field reaches a value of 1.03×10^{15} G, whereas the surface magnetic field was found to be 2.02×10^{14} G.

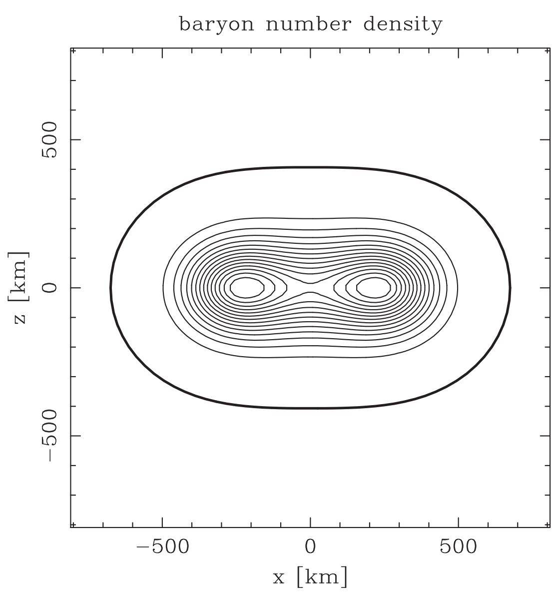

FIG. 2. Isocontours of the baryon number density in the (x,z) plane for the same star as shown in Fig. 1. The central baryon density for this model is 1.679×10^{-5} fm^{-3} (2.79×10^{10} g/cm^3).

The figure illustrates that the Lorentz force exerted by the magnetic field breaks the spherical symmetry of the star considerably and acts as a centrifugal force that pushes the matter off center. For a better understanding of this aspect, we use the equation of motion (10) for the static case, $\Gamma = 0$,

$$H(r,\theta) + \nu(r,\theta) + M(r,\theta) = C, \tag{14}$$

and plot these quantities in the equatorial plane as shown in Fig. 3. This same analysis was presented for magnetized neutron stars in Ref. [17]. The constant C can be calculated at every point in the star. We have chosen the center, since the central value of the magnetic potential $M(r,\theta)$ is zero and the central enthalpy H_c is our input to construct solutions. The Lorentz force is the derivative of the magnetic potential $M(r,\theta)$ in Eq. (14) and reaches its maximum value off center ($r_{\rm eq} \sim 350$ km, see Fig. 3). As already discussed in Ref. [17], the direction of the magnetic forces in the equatorial plane depends on the current distribution inside the star. In addition, the magnetic field changes its direction in the equatorial plane and, therefore, the Lorenz force reverses the direction inside the star. In our case, this can be seen from the qualitative change in behavior of the function $M(r,\theta)$ around $r_{\rm eq} \sim 350$ km in Fig. 3.

In order to compare our results with those in the literature, we compute the mass-radius diagram for magnetized white dwarfs shown in Fig. 4. As pointed out in Ref. [41], a fully consistent equilibrium configuration for magnetized white dwarfs is still lacking. The same authors have used a relativistic framework with cylindrical coordinates and the splitting of the pressure into parallel and perpendicular components to show that the maximum magnetic field inside these objects cannot exceed 1.5×10^{13} G. Their solutions also indicate that it is not possible to have stable magnetized WDs with super-Chandrasekhar masses. The maximum magnetic field strength obtained in Ref. [41] is less than the value obtained by a self-consistent solution of Newtonian white dwarfs as presented in Ref. [14], and orders of magnitude less than predicted in Ref. [25]. However, as discussed in Refs. [33–35], the paper [25] has been criticized above all because their calculation violates both macro-/microphysics properties essential for the stability of these objects.

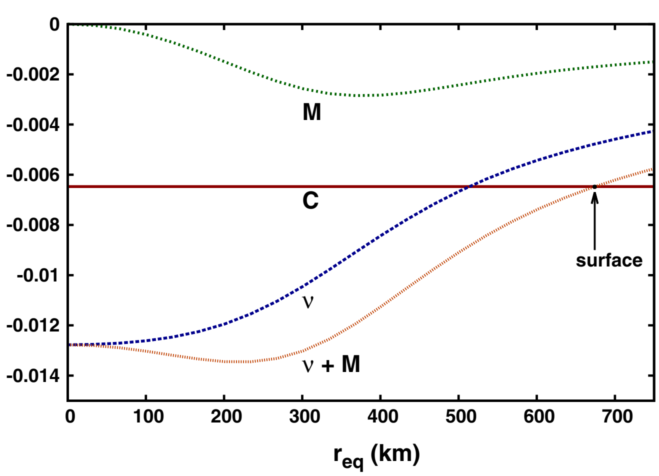

FIG. 3 (color online). Behavior of the different terms of the equation of motion as a function of the equatorial coordinate radius for the same star as shown in Fig. 1.

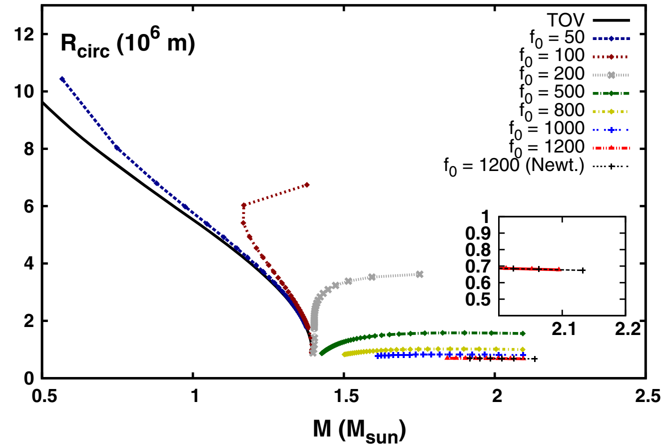

FIG. 4 (color online). Mass-radius diagram for magnetized white dwarfs. Different curves represent different values of the current function f_0. We also compare the maximum white dwarf mass obtained in the Newtonian case (in black) and in the relativistic one (in red) for the maximum electric current value for which numerical convergence is achieved. This diagram is quite similar to the MR diagram calculated in Ref. [14]. However, those authors have evaluated only Newtonian white dwarfs. All curves in this figure were calculated for a ratio between the magnetic and matter pressure less than or quite close to 1 at the center of the star.

In Fig. 4, the maximum white dwarf masses are obtained when the ratio between the magnetic and the matter pressure at the center of the star is less than or about 1. For such a strong magnetic field, the magnetic force has pushed the matter off center and a topological change to a toroidal configuration can take place [17]. This gives a limit for the magnetic field strength that can be computed within this approach, since our current numerical tools do not enable us to handle toroidal configuration.

The maximum masses of white dwarfs increase with stronger magnetic field. In our calculation, we found a mass for a relativistic white dwarf of 2.09 $M_\odot$ for almost the same magnetic field strength at the center, $B \sim 10^{14}$ G, as in Ref. [14]. The same authors presented configurations with magnetic fields up to 10^{16} G, which we have not found in our calculations. In the Newtonian case, we found a mass of 2.13 $M_\odot$ for the most massive magnetized white dwarf. In both cases, the masses are well above the Chandrasekhar limit of 1.4 $M_\odot$.

IV. ROTATING MAGNETIZED WHITE DWARFS

Besides magnetic fields, rotation is a crucial observable in stellar astrophysics. Typically, white dwarfs can rotate with periods of days or even years. On the other hand, according to Ref. [42], one of the fastest observed WDs possesses a spin period of 13.2*s*, a value similar to the ones observed in soft gamma repeaters (SGRs) and anomalous x-ray pulsars (AXPs), known as magnetars [43,44]. A relation between white dwarfs and magnetars was addressed in Ref. [45], where the authors speculated that SGRs and AXPs with low magnetic field on the surface might be rotating magnetized white dwarfs.

Rigidly rotating nonmagnetized white dwarfs were already studied a long time ago in the Newtonian framework [46–51]. In addition, the structure of rapidly rotating white dwarfs was performed in general relativity as in Ref. [52], and more recently in Ref. [53], where the authors used Hartle's formalism [54] to solve the approximate Einstein equations. It is obvious that all rotating stars have to satisfy the mass shedding, or Keplerian limit, as a condition of stability. This limit is reached when the centrifugal force due to rotation does not balance gravity anymore and the star starts to lose particles from the equator, defining an upper limit to the angular velocity of uniformly rotating stars.

In the same way that rotation provides a natural limit for the stability of stars, in the case of WDs, there are also microphysics aspects, as for example, the inverse β-decay and pycnonuclear fusion reactions [33,34,40], which need to be taken into account for a complete and self-consistent description of these stars. In this paper, however, we restrict ourselves to the study of the combined effect of rotation and magnetic fields on the global structure of WDs and we do not address these microphysics aspects.

In Fig. 5, we depict the Tolman-Oppenheimer-Volkoff (TOV) solution for the structure of a spherically symmetric white dwarf and the mass-shedding frequency limit. The centrifugal force exerted by the rotation acts against gravity, which allows the star to support higher masses compared to the static case. In the first place, by comparison of Figs. 4 and 5, one sees that magnetic fields are more efficient than rotation in increasing the maximum mass of stars. The maximum mass obtained for a relativistic and magnetic white dwarf is 2.09 $M_\odot$, whereas the maximum mass achieved by rotation is $\sim$1.45 $M_\odot$.

The relation between the Keplerian frequency (f_K) and the central density of the star is displayed in Fig. 6. With higher angular velocity, the centrifugal forces increase, pushing the matter outward, therefore acting against gravity. As a result, the stars are allowed to have more mass, increasing the central density. This is possible, because the centrifugal forces due to rotation ($f_c \propto r\Omega^2$) have much more effect on the outer layers of the star. On the other hand, for nonrotating magnetized stars, the Lorenz force acts mainly in the inner layers of the star, reducing, and not increasing, the central densities in these objects as shown in Ref. [18].

Henceforth we investigate the role played by the magnetic field in uniformly rotating white dwarfs. For a star with central enthalpy of $H_c = 0.005c^2$, whose mass is close to the maximum mass in the static case, we present results for three different calculations: (A) static and nonmagnetized; (B) rotating (with the Keplerian frequency) and nonmagnetized and (C) rotating (with the Keplerian frequency) and magnetized. Cases (A) and (B) are presented in the mass-radius diagram in Figs. 4 and 5. For case (B), the star rotates with its Keplerian frequency of 0.99 Hz. In addition, in order to compute stellar solutions for the case (C), we turn on the magnetic field until the limit of numerical convergence is reached. The resulting magnetic field lines and the electric isopotential lines $A_t =$ const are depicted in Fig. 7. In order to study how the Keplerian

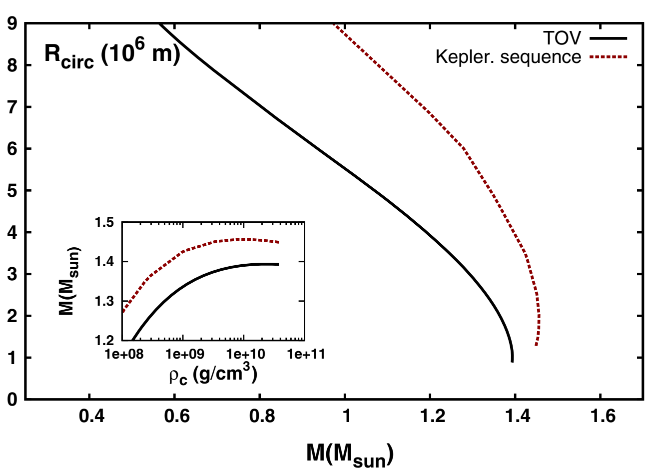

FIG. 5 (color online). Mass-radius diagram for static and rotating white dwarfs. The TOV solution is shown in black, and the red (dotted) curve indicates the Keplerian sequence for rotating WDs. In the bottom left-hand corner the gravitational mass as a function of the central density for the same sequence of stars is shown.

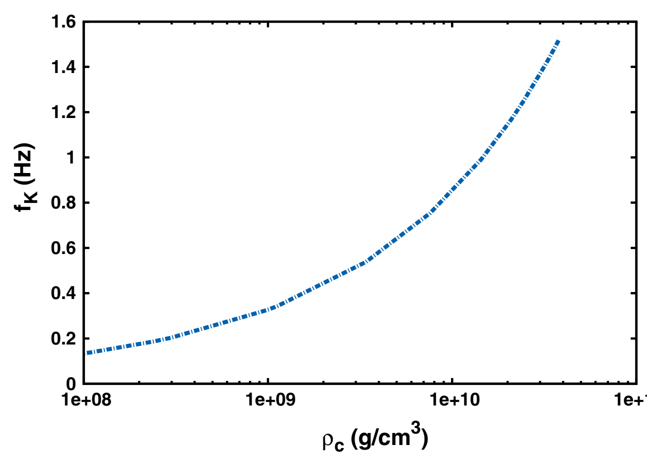

FIG. 6 (color online). Keplerian frequency as a function of the central baryon density for the sequence as shown in Fig. 5. The maximum frequency reached by a nonmagnetized and uniformly rotating white dwarf is 1.52 Hz.

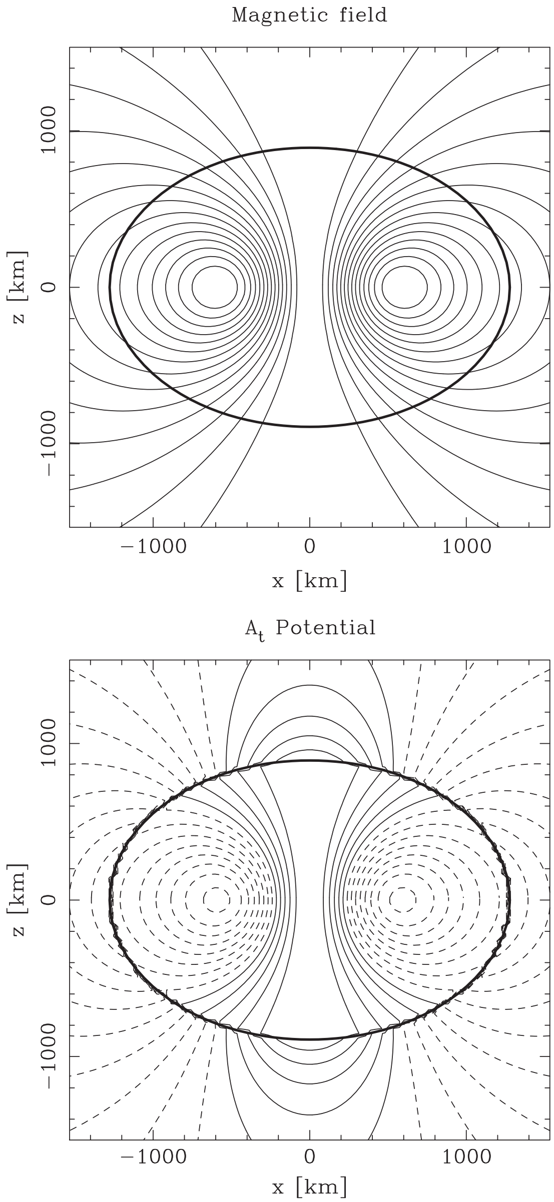

FIG. 7. Magnetic field lines (up) and electromagnetic potential lines (down) for a star with $H_c = 0.005c^2$ and gravitational mass of $\sim$1.57 $M_{\odot}$, with a Keplerian frequency of 1.13 Hz. The dipole magnetic moment reaches 6.93×10^{33} Am^2 and the magnetic field intensity at the center of this white dwarf is 1.87×10^{14} G.

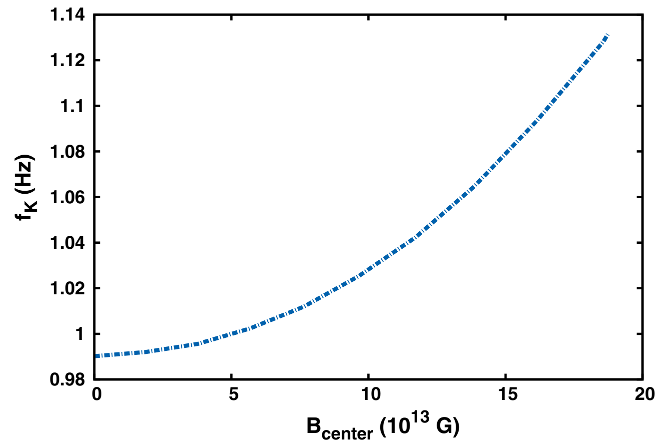

FIG. 8 (color online). Keplerian frequency as a function of the central magnetic field for the nonmagnetized (case B, i.e., $f_K = 0.99$ Hz) and the magnetized (case C, i.e., $f_K = 1.13$ Hz) white dwarfs.

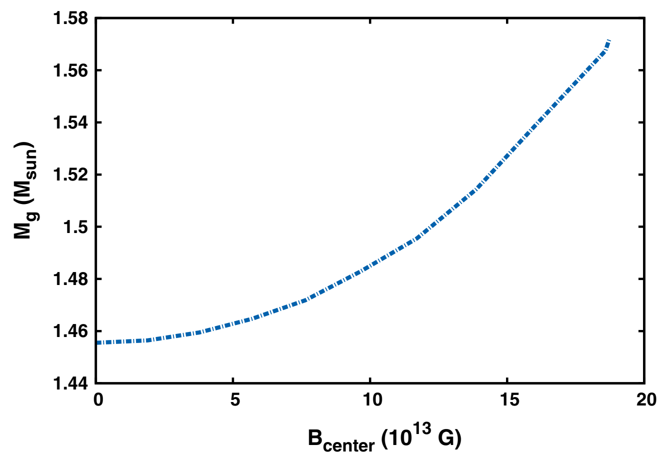

FIG. 9 (color online). Gravitational mass as a function of the central magnetic field for stars with central enthalpy $H_c = 0.005c^2$ for cases (B) and (C), which are the same stars as shown in Fig. 8.

frequency changes with the magnetic field, we perform a calculation for different current functions $f = f_0 = \text{const}$, from zero [case (B)] to the maximum value of the magnetic field as shown in Fig. 7. As a result, the Keplerian frequency increases with the magnetic field as shown in Fig. 8. In this way, equilibrium configurations are obtained for higher centrifugal forces and, therefore, if the star can rotate faster, in consequence it can support higher masses, which explains the behavior observed in Fig. 9.

According to Fig. 6, nonmagnetized white dwarfs can reach a maximum Keplerian frequency of 1.52 Hz. However, in the magnetic case (Fig. 8), the maximum Keplerian frequency is reduced to 1.13 Hz, which corresponds to a white dwarf with gravitational mass of $\sim$1.57 $M_{\odot}$ and a central magnetic field of 1.87×10^{14} G.

V. CONCLUSIONS

We computed perfect-fluid magnetized white dwarfs in general relativity by solving the coupled Einstein-Maxwell equations. We have applied a formalism that was developed for neutron stars to rotating magnetized white dwarfs. In our case, the equilibrium solutions are axisymmetric and stationary, including a strong poloidal magnetic field.

The observation of superluminous Ia supernovae suggests that their progenitors are super-Chandrasekhar white dwarfs, whose masses are higher than 1.4 $M_{\odot}$. The increase in mass may be a consequence of ultrastrong magnetic field inside the white dwarfs. The relevance of magnetic fields in enhancing the maximum mass of a white dwarf was studied and the results were obtained in a fully relativistic framework. We have shown that white dwarfs masses increase up to 2.09 $M_{\odot}$ for a maximum magnetic field strength of $\sim 10^{15}$ G in the stellar center. Thus, magnetic fields can, potentially, be responsible for super-massive white dwarfs.

The structure of relativistic, axisymmetric and uniformly rotating magnetized white dwarfs were investigated self-consistently and all effects of the electromagnetic fields on the star equilibrium were taken into account. Unsurprisingly, nonmagnetized configurations at the mass shedding limit support higher masses than their static counterparts. However, we have seen that the magnetic field is much more efficient in increasing the mass of WDs than rotation. For example, the Keplerian sequence has a maximum mass of ~ 1.45 $M_{\odot}$, whereas for the maximum magnetic field configuration achieved in this calculation, the maximum mass of relativistic WDs is 2.09 $M_{\odot}$, i.e., 33% larger than the Chandrasekhar limit, and 2.13 $M_{\odot}$ in the Newtonian framework.

We have also shown the increase of the Keplerian frequency (f_K) with the magnetic field. For stronger magnetic fields the Lorenz force increases, which, in turn, helps the star to support more mass than in the non-magnetized case. As a result, as these stars are more massive, they can rotate faster (see Figs. 8 and 9). In this case, the maximum mass obtained for rotating magnetized white dwarfs is ~ 1.57 $M_{\odot}$, with a Keplerian frequency of 1.13 Hz.

Note that purely poloidal or purely toroidal magnetic field configurations undergo intrinsic instabilities as suggested years ago in Refs. [55–58]. The nature of this instability was confirmed both in Newtonian numerical simulations in Refs. [59–62] and in a general relativity framework in Refs. [63–66]. Analytical and numerical calculations have also shown that stable equilibrium configurations are obtained for magnetic fields composed not only by a poloidal component, which extends throughout the star and to the exterior, but also a toroidal one, which is confined inside the star [61,67–70]. In addition, the magnetic field might decay due to Ohmic effects and, thereby, change its strength and distribution in the star [71]. In this study we have modeled magnetized white dwarfs with a purely poloidal magnetic field, which is not the most general case. However, using these restrictive assumptions we have shown, in a fully general relativity way, that magnetic field effects can considerably increase the star masses and, therefore, might be the source of superluminous SNIa. In future work, in order to have a more complete description of the stars presented here, we intend to take into account magnetic field configurations with both poloidal and toroidal components, a B-field dependent equation of state and effects of the anomalous magnetic moment.

ACKNOWLEDGMENTS

The authors thank Nicolas Chamel for fruitful comments on the onset of the electron capture by carbon-12 nuclei and the referee for the valuable comments and suggestions. B. Franzon acknowledges support from CNPq/Brazil, DAAD and HGS-HIRe for FAIR. S. Schramm acknowledges support from the HIC for FAIR LOEWE program.

[1] S. L. Shapiro and S. A. Teukolsky, *Black Holes, White Dwarfs and Neutron Stars: The Physics of Compact Objects* (John Wiley & Sons, New York, 2008).
[2] N. K. Glendenning, *Compact Stars: Nuclear Physics, Particle Physics and General Relativity* (Springer Science & Business Media, New York, London, 2012).
[3] R. H. Fowler, Mon. Not. R. Astron. Soc. **87**, 114 (1926).
[4] P. A. Dirac, in *Proceedings of the Royal Society of London A: Mathematical, Physical and Engineering Sciences* (The Royal Society, New York, London, 1926), Vol. 112, pp. 661–677.
[5] E. Fermi, Rend. Fis. Acc. Lincei **3**, 145 (1926).
[6] S. Chandrasekhar, Astrophys. J. **74**, 81 (1931).
[7] S. Chandrasekhar, *An Introduction to the Study of Stellar Structure* (University of Chicago Press, Chicago, 1939).
[8] Y. Terada, T. Hayashi, M. Ishida, K. Mukai, T. u. Dotani, S. Okada, R. Nakamura, S. Naik, A. Bamba, and K. Makishima, Publ. Astron. Soc. Jpn. **60**, 387 (2008).
[9] D. Reimers, S. Jordan, D. Koester, N. Bade, T. Kohler, and L. Wisotzki, Astron. Astrophys. **311**, 572 (1996).
[10] G. D. Schmidt and P. S. Smith, Astrophys. J. **448**, 305 (1995).
[11] J. C. Kemp, J. B. Swedlund, J. D. Landstreet, and J. R. P. Angel, Astrophys. J. **161**, L77 (1970).
[12] A. Putney, Astrophys. J. **451**, L67 (1995).
[13] J. Angel, Annu. Rev. Astron. Astrophys. **16**, 487 (1978).
[14] P. Bera and D. Bhattacharya, Mon. Not. R. Astron. Soc. **445**, 3951 (2014).
[15] M. Bocquet, S. Bonazzola, E. Gourgoulhon, and J. Novak, Astron. Astrophys. **301**, 757 (1995).
[16] D. Chatterjee, T. Elghozi, J. Novak, and M. Oertel, Mon. Not. R. Astron. Soc. **447**, 3785 (2015).
[17] C. Y. Cardall, M. Prakash, and J. M. Lattimer, Astrophys. J. **554**, 322 (2001).
[18] B. Franzon, V. Dexheimer, and S. Schramm, arXiv: 1508.04431.
[19] R. A. Scalzo *et al.*, Astrophys. J. **713**, 1073 (2010).
[20] D. A. Howell *et al.* (SNLS Collaboration), Nature (London) **443**, 308 (2006).

[21] M. Hicken, P. M. Garnavich, J. L. Prieto, S. Blondin, D. L. DePoy, R. P. Kirshner, and J. Parrent, Astrophys. J. **669**, L17 (2007).
[22] M. Yamanaka *et al.*, Astrophys. J. **707**, L118 (2009).
[23] S. Taubenberger, S. Benetti, M. Childress, R. Pakmor, S. Hachinger, P. Mazzali, V. Stanishev, N. Elias-Rosa, I. Agnoletto, F. Bufano *et al.*, Mon. Not. R. Astron. Soc. **412**, 2735 (2011).
[24] R. Moll, C. Raskin, D. Kasen, and S. Woosley, Astrophys. J. **785**, 105 (2014).
[25] U. Das and B. Mukhopadhyay, Phys. Rev. D **86**, 042001 (2012).
[26] U. Das and B. Mukhopadhyay, Phys. Rev. Lett. **110**, 071102 (2013).
[27] U. Das and B. Mukhopadhyay, J. Cosmol. Astropart. Phys. 06 (2014) 050.
[28] D. Adam, Astron. Astrophys. **160**, 95 (1986).
[29] J. P. Ostriker and P. Bodenheimer, Astrophys. J. **151**, 1089 (1968).
[30] J. P. Ostriker and F. Hartwick, Astrophys. J. **153**, 797 (1968).
[31] J. P. Ostriker and J. L. Tassoul, Astrophys. J. **155**, 987 (1969).
[32] S. Subramanian and B. Mukhopadhyay, arXiv:1507.01606.
[33] J. G. Coelho, R. M. Marinho, M. Malheiro, R. Negreiros, D. L. Cáceres, J. A. Rueda, and R. Ruffini, Astrophys. J. **794**, 86 (2014).
[34] N. Chamel, A. F. Fantina, and P. J. Davis, Phys. Rev. D **88**, 081301 (2013).
[35] R. Nityananda and S. Konar, Phys. Rev. D **91**, 028301 (2015).
[36] S. Bonazzola, E. Gourgoulhon, M. Salgado, and J. Marck, Astron. Astrophys. **278**, 421 (1993).
[37] E. Gourgoulhon, *3+1 Formalism in General Relativity: Bases of Numerical Relativity* (Springer Science & Business Media, New York, London, 2012), Vol. 846.
[38] A. Lichnerowicz, Southwest Center for Advanced Studies and The Mathematical Physics Monograph Series, *Relativistic Hydrodynamics and Magnetohydrodynamics* (W.A. Benjamin, New York, 1967), Vol. 35.
[39] I.-S. Suh and G. Mathews, Astrophys. J. **530**, 949 (2000).
[40] N. Chamel and A. F. Fantina, Phys. Rev. D **92**, 023008 (2015).
[41] D. M. Paret, A. P. Martinez, and J. Horvath, arXiv: 1501.04619.
[42] S. Mereghetti, A. Tiengo, P. Esposito, N. La Palombara, G. L. Israel, and L. Stella, Science **325**, 1222 (2009).
[43] R. C. Duncan and C. Thompson, Astrophys. J. **392**, L9 (1992).
[44] C. Thompson and R. C. Duncan, Astrophys. J. **408**, 194 (1993).
[45] M. Malheiro and J. G. Coelho, in *Proceedings of the 13th Marcel Grossmann Meeting on Recent Developments in Theoretical and Experimental General Relativity, Astrophysics, and Relativistic Field Theories (MG13)* (World Scientific, Stockholm University, Sweden, 2012), pp. 2462–2464.
[46] S. Krishan and R. Kushwaha, Publ. Astron. Soc. Jpn. **15**, 253 (1963).
[47] S. Anand, Proc. Natl. Acad. Sci. U.S.A. **54**, 23 (1965).
[48] R. James, Astrophys. J. **140**, 552 (1964).
[49] I. Roxburgh and B. Durney, Z. Astrophys. **64**, 504 (1966).
[50] J. Monaghan, Mon. Not. R. Astron. Soc. **132**, 305 (1966).
[51] V. Geroyannis and A. Hadjopoulos, Astrophys. J. Suppl. Ser. **70**, 661 (1989).
[52] G. Arutyunyan, D. Sedrakyan, and É. Chubaryan, Sov. Astron. **15**, 390 (1971).
[53] K. Boshkayev, J. A. Rueda, R. Ruffini, and I. Siutsou, Astrophys. J. **762**, 117 (2013).
[54] J. B. Hartle, Astrophys. J. **150**, 1005 (1967).
[55] P. Markey and R. Tayler, Mon. Not. R. Astron. Soc. **163**, 77 (1973).
[56] R. Tayler, Mon. Not. R. Astron. Soc. **161**, 365 (1973).
[57] G. Wright, Mon. Not. R. Astron. Soc. **162**, 339 (1973).
[58] E. Flowers and M. A. Ruderman, Astrophys. J. **215**, 302 (1977).
[59] S. K. Lander and D. Jones, Mon. Not. R. Astron. Soc. **424**, 482 (2012).
[60] J. Braithwaite, Astron. Astrophys. **453**, 687 (2006).
[61] J. Braithwaite and Å. Nordlund, Astron. Astrophys. **450**, 1077 (2006).
[62] J. Braithwaite, Astron. Astrophys. **469**, 275 (2007).
[63] R. Ciolfi and L. Rezzolla, Mon. Not. R. Astron. Soc. Lett. **435**, L43 (2013).
[64] P. D. Lasky, B. Zink, K. D. Kokkotas, and K. Glampedakis, Astrophys. J. Lett. **735**, L20 (2011).
[65] P. Marchant, A. Reisenegger, and T. Akgün, Mon. Not. R. Astron. Soc. **415**, 2426 (2011).
[66] J. Mitchell, J. Braithwaite, A. Reisenegger, H. Spruit, J. Valdivia, and N. Langer, Mon. Not. R. Astron. Soc. **447**, 1213 (2015).
[67] C. Armaza, A. Reisenegger, and J. A. Valdivia, Astrophys. J. **802**, 121 (2015).
[68] K. H. Prendergast, Astrophys. J. **123**, 498 (1956).
[69] J. Braithwaite and H. C. Spruit, Nature (London) **431**, 819 (2004).
[70] T. Akgün, A. Reisenegger, A. Mastrano, and P. Marchant, Mon. Not. R. Astron. Soc. **433**, 2445 (2013).
[71] P. Goldreich and A. Reisenegger, Astrophys. J. **395**, 250 (1992).